CrossMark

Optimization and predictive modeling using S/N, RSM, RA and ANNs for micro-electrical discharge drilling of AISI 304 stainless steel

Murat Sarıkaya[1] · Volkan Yılmaz[2]

Abstract In present work, micro-deep holes on AISI 304 stainless steel were drilled via electrical discharge machining (EDM) method. In the first phase of this work, the effect of test parameters on the drilling performance and the profile of drilled holes were investigated experimentally. Test parameters including discharge current, dielectric spray pressure and electrode tool rotational speed were taken and then the machining rate (MR), electrode wear rate (EWR), average over-cut (AOC) and taper angle (TA) were measured in order to assess the drillability of EDM. After experimental study, an analysis of variance was performed to identify the effect of the importance of test parameters on experiment outputs. In the second phase of this study, optimum process parameters were determined using signal-to-noise analysis and response surface methodology (RSM) for mono-optimization and multi-response optimization, respectively. In the last phase, regression analysis and artificial neural network (ANN) models for predicting the MRR, EWR, AOC and TA. As a result of experimental analysis, discharge current was the most important parameter for micro-drilling with EDM. It was found out that this parameter influenced positively MR, while it has negatively an effect on EWR, AOC and TA. Mathematical model based on ANNs exhibited a successful performance for predication of outputs. Optimum process parameters which were discharge current of 10.18 Å, dielectric liquid pressure of 58.78 bar and electrode tool rotational speed of 100 rpm for multi-objective optimization were determined through RSM with desirability function analysis in micro-deep hole EDM drilling of AISI 304 stainless steel.

1 Introduction

In order to obtain a better corrosion resistance, low thermal conductivity and high strength in the high-temperature working conditions, AISI 304 stainless steel has been developed. Due to its superior characteristics, this steel has been widely employed for many fields such as medical, defense, chemical, construction and aerospace industry. However, the machining of stainless steel with traditional methods is very difficult compared to carbon steel. In the machining operations, the drilling of workpiece has an important position because more than 40% metal cutting operations are the drilling of workpiece [1, 2]. In many fields, with shrinking the size of mechanical system, hole diameters are reduced and so demand for micro-holes has further increased. However, recently holes in micro-diameter and high length have been extremely difficult to obtain by using traditional cutting processes and even obtaining the smaller holes than 1 mm has become almost impossible. Apart from traditional cutting processes, alternative production methods including laser machining, focused ion beam machining, electro-chemical machining and electrical discharge machining (EDM) or electrical discharge drilling (EDD) are employed for micro-part manufacturing [3]. In these methods, recently drilling with electrical

✉ Murat Sarıkaya
msarikaya@sinop.edu.tr

1 Department of Mechanical Engineering, Sinop University, 57030 Sinop, Turkey

2 Department of Manufacturing Engineering, Technology Faculty, Gazi University, 06500 Ankara, Turkey

discharge drilling method has been used as an alternative machining option in order to easily drill the smaller diameter holes. Through this method without mechanical contact with the workpiece, forming can be made to achieve a product with help of the electrical conductivity of workpiece material [4]. In electrical discharge drilling, there is not any effect of mechanical properties of the materials that are very important for traditional cutting processes on the machinability of workpiece. In crucial fields such as aerospace, automotive, medicine, manufacturing and defense industry so as to drill the holes desired micro-diameter and length, this method has become an important option. Fundamental expectation in drilling operations with EDM is to obtain economical and accurate hole geometry and size. In some studies, the drillability of workpiece with electrical discharge machining method was investigated by researchers. For example, Volkan et al. [4] investigated deep-micro-hole drilling for Hadfield steel by electro-discharge machining. It was found that the most effective variable affecting the MRR, EWR and RW was the discharge current. Kuppan et al. [5] examined the effect of input values for deep hole drilling of Inconel 718. It was seen that while the machining rate was affected by peak current, duty factor and electrode rotation, the surface roughness was affected by peak current and pulse on-time. Ay et al. [6] optimized test input parameters for micro-drilling of Inconel 718 with EDM. Asokan et al. [7] analyzed the influence of test parameters on performance characteristics in EDM-deep-hole drilling of titanium alloy. Mohan et al. [8, 9] investigated the machinability for electrical discharge machining of Al–SiC metal matrix composite. Puertas et al. [10] investigated the effect of experiment parameters on surface quality, MRR and EW of WC–Co in EDM operation. Lee et al. [11] made electrode wear estimation model for EDM drilling. Plaza et al. [12] carried out an experimental study for micro-EDM drilling of Ti–6Al–4V with help of helical electrode. Jahan et al. [13] studied the drillability of deep-micro-holes for two difficult-to-machine materials such as cemented carbide and austenitic stainless steel via micro-EDM method. Pradhan et al. [14] presented a research in order to optimize micro-EDM test parameters in machining of Ti–6Al–4V superalloy. Wang et al. [15] explored the micro-hole drilling process for PCDs with micro-electrical discharge machining. From the literature survey, it is detected that although a lot of studies have been performed for drilling process with EDM, there is not any study for micro-deep-hole drilling of AISI 304 stainless steel with electrical discharge machining method.

Today's industry desires to manufacture the high-quality products with low cost in a shorter time. In order to achieve this goal of industry process, parameters have to be optimized by taking into consideration all quality outputs [16].

In engineering applications, there are a lot of tools used by researchers for optimization such as Taguchi method, gray relational analysis (GRA), response surface methodology (RSM) and genetic algorithm. Recently, RSM has been applied by researchers [17–20] in order to optimize multi-response problems for engineering processes because some tools cannot determine simultaneously the best combination of input parameters for multiple response outputs. Although in traditional cutting processes there are many studies about optimization with RSM, there is not any investigation focused on the optimization of multiple response outputs in micro-deep electrical discharge drilling with help of RSM.

Due to the complexity of the cutting process, researchers have more focused on predictive modeling tools in order to detect a result of quality indicator without an experiment performed [21]. There are several predictive modeling tools including regression analysis, artificial neural networks (ANNs) and fuzzy logic so as to establish a relationship between input parameters and output(s) parameter.

In the light of the above information, current study aims to explore the deep-micro-hole drilling of AISI 304 stainless steel through micro-electrical discharge machining method. For this aim, the discharge current, dielectric spray pressure and electrode tool rotational speed which measured in this study were taken as process parameters in order to evaluate their effects on machining rate, electrode wear rate, average over-cut and taper angle during deep-micro-hole drilling of AISI 304 material. After experimental study in order to achieve simultaneously the desired results in terms of all responses, the micro-EDM process parameters were optimized by using RSM based on multiple performance outputs. Further, present study focused on predictive models via artificial neural networks and regression analysis so as to assign a relationship between process parameters and performance characteristics. Additionally, analysis of variance (ANOVA) was also applied in order to identify the contribution rates of test parameters on quality characteristics.

2 Experimental setup

2.1 Materials and machine tool

The workpiece material used in current study was AISI 304 austenitic stainless steel, and its size was $X = 100$ mm, $Y = 10$ mm and $Z = 20$ mm block material. Brass electrode which is usually used for drilling operations was chosen as tool material because it is more economical compared to copper and tungsten tools. In addition, brass tools can also become resistant to high tensile compared with copper tools [14]. The total length, outside diameter

and inside diameter of electrode used in present study were 400 mm, 500 μm and 180 μm, respectively. Pure water was utilized as dielectric fluid during drilling process. Dielectric liquid was pumped to the machining region passing through the interior section of the electrode. In order to make the micro-drilling experiments the "Furkan" brand, "EEI M50A" type EDM machine was employed. A power unit was also added to system so as to give desired spindle speed to electrode tool in rotations per minute.

2.2 Experimental procedure

Before the experiments began, the top and bottom faces of workpiece material were machined using CNC vertical milling machine. In experiments, discharge current, dielectric spray pressure and electrode tool rotational speed were taken as process parameters by keeping other factors constant. Detailed information about machining parameters and their levels were given in Table 1. A photographic image of the experimental setup designed for the tests is seen in Fig. 1. The pressure head was combined with moving part of the EDM machine along the Z-axis. A rotational motion was provided through pressure head and the pressurized dielectric liquid reached machining region via electrode. The rotational motion of electrode was achieved with a DC motor on the pressure head. The dielectric liquid reached the pressure head with the help of a pressure pump. The dielectric liquid pressure was controlled with a manometer on the bypass mechanism at any moment. The experiments were conducted on a separate working tank mounted inside the original tank of the machine. The materials inside the working tank were fastened with a clamp. In order to prevent the electrode set from turning eccentrically, it was placed near the test samples through the ceramic guide.

2.3 Measurements

Micro-deep hole drilling performance was evaluated by machining rate (MR), electrode wear rate (EWR), the accuracy of the holes including average over-cut (AOC) and taper angle (TA). MR and EWR were determined by calculating the weight difference between of tool and workpiece material before and after drilling per-unit machining time in each experiment. In order to measure the weight for electrode and workpiece material, a
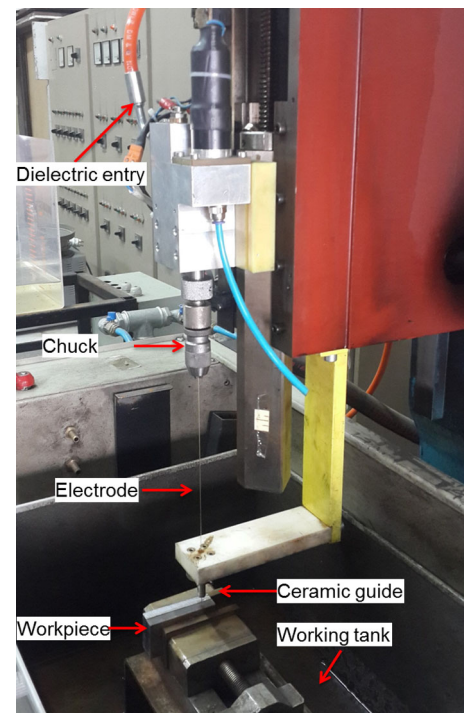

Fig. 1 Experimental setup for micro-EDM drilling tests

sensitive balance having sensitivity of 0.005 g was used. In order to determine the hole diameter and dimensions and to examine the hole diameter, finished samples were dried, cleansed and later scanned on a high-resolution scanner. Later, these images were used to measure the diameters of each hole using image analysis package software. Figure 2 shows the schematic diagram of calculating average over-cut and taper angle. In this figure, AOC and TA of the machined micro-hole with electrical discharge machining were calculated by Eqs. (1) and (2) as follows:

$$AOC = \frac{\frac{(d_1 + d_2 + d_3 + d_4 + d_5 + d_6 + d_7)}{7} - \text{tool diameter}}{2} \quad (1)$$

where AOC is average over-cut and $d_1, d_2, d_3, \ldots, d_n$ are hole diameters measured at different points.

$$TA(\theta) = \tan^{-1}\left(\frac{d_{id} - d_{od}}{2 \times L}\right) \quad (2)$$

where TA is hole taper angle, d_{id} is hole entry diameter, d_{od} is hole exit diameter, and L is hole depth.

Table 1 EDM-drilling parameters

Parameter	Notation	Unit	Level 1	Level 2	Level 3
Discharge current	I	Ampere	6	12	24
Dielectric liquid pressure	P	Bar	20	40	80
Too rotational speed	N	rpm	100	200	400
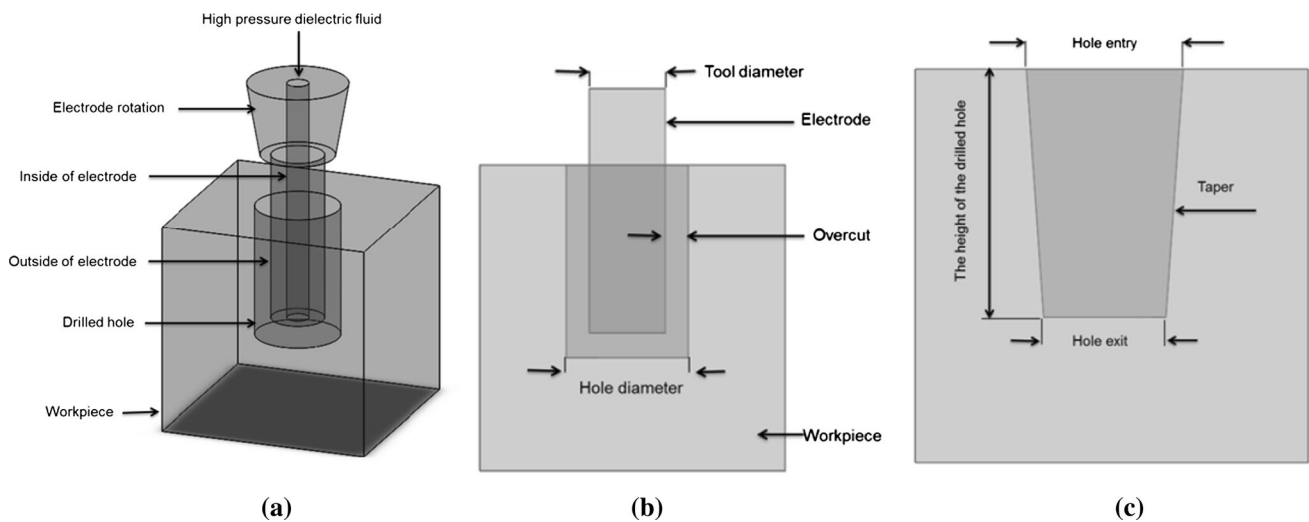
Fig. 2 EDM drilling procedure. **a** General form, **b** over-cut and **c** taper angle

3 Results and discussion

Design of experiment and tests results are shown in Table 2.

3.1 Machining rate

In EDM operations, machining rate (MR) is an important process parameter for which higher valued results are preferred. Figure 3 shows the values obtained for MR corresponding to various machining parameters in this study, where the focus is on micro-hole drilling in AISI 304 type stainless steel material. An analysis of Fig. 3 indicates a distinct increase in MR values in response to increase in discharge current. This result is due to the increase in discharge energy as discharge current is increased. With increased discharge energy, more material is melted and vaporized in unit time from the surface of the workpiece material. As sparking is more powerful due to the increased discharge current, more material is melted and vaporized per spark compared to that observed in case of lower discharge current [22]. Accordingly, the value for MR, which corresponds to weight of material removed per unit time, is increased in parallel to increased discharge current values. In this study, the average MR value increased by 273% when discharge current value increased from 6 to 12 Å, and the average MR value increased by 150% when discharge current increased from 12 to 24 Å.

Further analysis of Fig. 3 indicates a distinct increase in MR values in response to increase in electrode tool rpm values. The average MR value increased by 8.7% when the electrode tool rpm value increased from 100 to 200 rev/min, and the average MR value increased by 5.7% when the electrode tool rpm value increased from 200 to 400 rev/min.

A similar outcome holds true for the full range of tests involving dielectric spray pressure. MR values have increased in response to increased dielectric spray pressure, albeit at different percentages. Figure 3 illustrates this outcome, indicating a clear increase in MR values in relation to dielectric spray pressure. The average MR value increased by 33% when the dielectric spray pressure increased from 20 to 40 bars, and the average MR value increased by 7.7% when the dielectric spray pressure increased from 40 to 80 bars.

The increase in MR values resulting from a combination of increases in electrode tool rpm and dielectric spray pressure is due to the rapid circulation of the dielectric fluid in the machining region, leading to sustained spark discharge in the same region. Sustained spark discharge has enabled uninterrupted machining, making sustained spark discharge the most effective cause for the observed increase in MR values.

Using through the tool delivery of the dielectric fluid spray enabled its faster removal from the lateral gaps between the electrode tool and the workpiece, resulting in more effective flushing, also described in the literature [23, 24].

In the study, increases in both electrode rotation rpm as well as dielectric spray pressure were found to increase MR values when machining AISI-304 type stainless steel material. The resulting increase has been significant in terms of machining performance and savings, allowing the drilling of micro-holes to be completed in shorter durations.

3.2 Electrode wear rate

Electrode wear rate (EWR) values are significant performance indicators in EDM operations. The EWR value

Table 2 Design of experiment and test results

Test number	Control factors			Test results			
	I (Å)	P (bar)	N (rpm)	MR (mg/min)	EWR (mg/min)	AOC (μm)	TA (°)
1	6	20	100	2.601	0.389	30	0.075057
2	6	20	200	3.548	0.423	44	0.080214
3	6	20	400	3.982	0.442	49	0.081360
4	6	40	100	5.500	0.376	36	0.069385
5	6	40	200	6.579	0.406	47	0.080787
6	6	40	400	6.849	0.431	52	0.083079
7	6	80	100	8.462	0.304	40	0.079641
8	6	80	200	9.524	0.359	56	0.085371
9	6	80	400	9.934	0.393	59	0.075917
10	12	20	100	18.214	5.357	78	0.177616
11	12	20	200	20.182	5.545	86	0.183403
12	12	20	400	21.143	6.286	92	0.189075
13	12	40	100	21.333	5.000	80	0.177960
14	12	40	200	23.750	5.188	87	0.188502
15	12	40	400	27.750	5.870	94	0.194805
16	12	80	100	23.667	4.270	85	0.183518
17	12	80	200	26.667	5.167	87	0.185867
18	12	80	400	28.742	5.839	93	0.188044
19	24	20	100	45.455	20.455	152	0.343771
20	24	20	200	47.500	22.500	168	0.379006
21	24	20	400	48.837	25.930	175	0.392470
22	24	40	100	59.375	20.125	155	0.395335
23	24	40	200	64.305	21.600	170	0.396767
24	24	40	400	66.285	22.500	185	0.398199
25	24	80	100	61.538	18.615	158	0.394762
26	24	80	200	65.455	20.455	187	0.393902
27	24	80	400	69.231	21.915	190	0.402210

Fig. 3 Surface plot of MR (mg/min) versus I (Å), P (bar) and N (rpm)
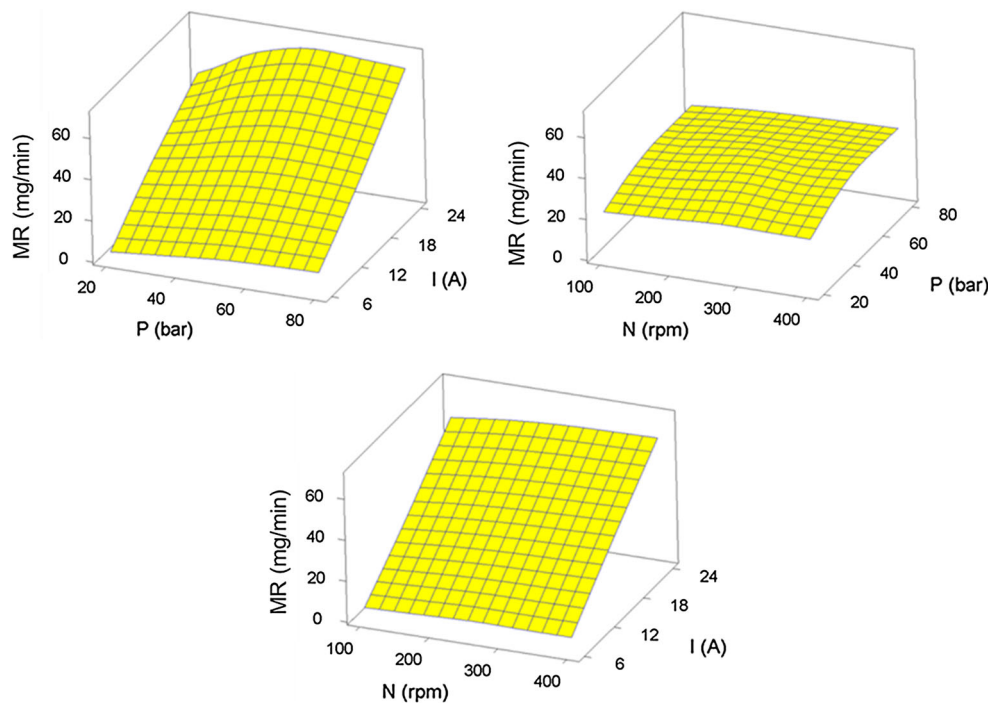
Fig. 4 Surface plot of EWR
(mg/min) versus I (Å), P (bar)
and N (rpm)
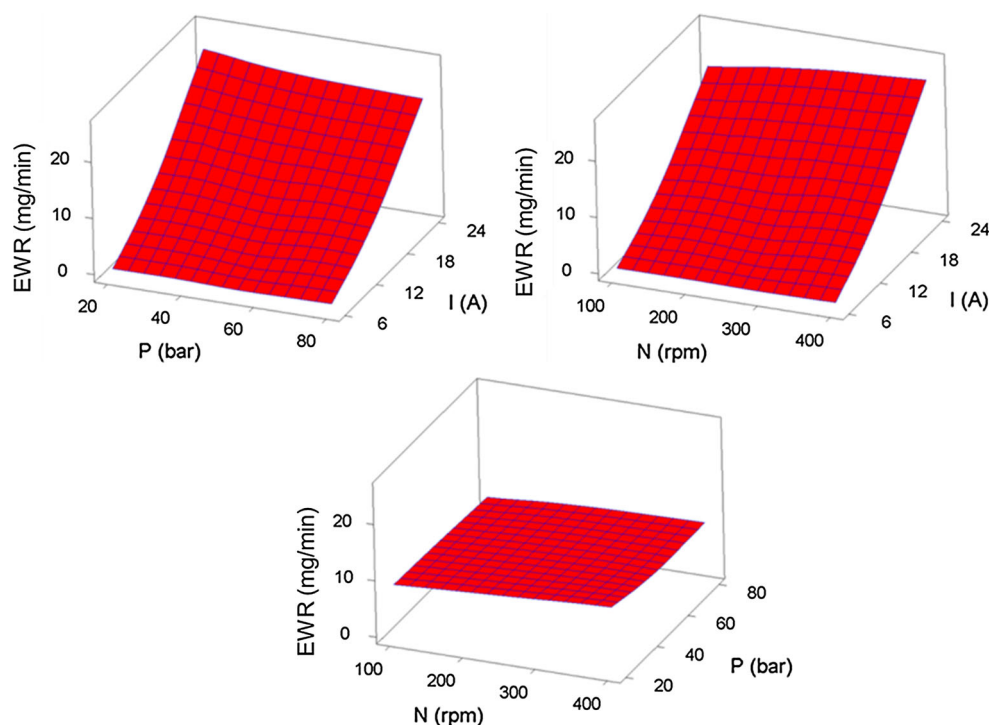
indicates the weight of electrode melted and vaporized per unit time, and a lower EWR value is an important indicator for higher efficiency and practical applicability of the machining process.

Figure 4 shows graphical depictions of EWR values obtained during the micro-hole drilling of AISI-304 type stainless steel material using brass cylindrical electrodes with outer diameter of 0.5 mm and inner diameter of 0.18 mm. Analysis of Fig. 4 indicates that EWR values increase in parallel to increased values of discharge current. In relation to the discharge current applied, each spark causes increased material to be melted and vaporized from the material being machined, and in parallel, a proportionally larger region was melted and vaporized from the electrode tool itself. As a result, EWR values are increased as discharge current is increased.

In this study, the average EWR value increased by 1282% when discharge current value increased from 6 to 12 Å, and the average EWR value increased by 300% when discharge current increased from 12 to 24 Å.

The average EWR value increased by 9% when the electrode tool rpm value (a process input parameter) increased from 100 to 200 rev/min, and the average EWR value increased by 9.7% when the electrode tool rpm value increased from 200 to 400 rev/min. The increased electrode tool rpm has led to a faster circulation of the dielectric fluid in the machining region, enabling increased sparking per unit time, which in turn has led to increased EWR values [22, 23].

In this study, decreased EWR values have been observed in relation to increases in dielectric spray pressure. The average EWR value decreased by 6.7% when the dielectric spray pressure increased from 20 to 40 bars, and the average EWR value decreased by 5.1% when the dielectric spray pressure increased from 40 to 80 bars. This decrease in EWR values observed in relation to increased dielectric spray pressure is interpreted to be due to the more effective means of washing and cooling that were enabled. Thanks to the spraying realized through the electrode tool, the electrode has been cooled more rapidly and the machining region has been flushed much more effectively, thereby preventing the occurrence of random sparking [24, 25]. Accordingly, EWR values have decreased in response to the higher dielectric spray pressures that have been utilized.

3.3 Average over-cut and taper angle

In EDM micro-hole drilling operations, average over-cut (AOC) is expressed as the variance between the diameter of the resulting hole and the diameter of the electrode tool, and indicates the gap between the electrode and the walls of the hole. A low AOC value is preferred (and ideally would approach zero), such that the hole diameter is equal to the electrode tool diameter.

In this study for micro-hole drilling in AISI-304 type stainless steel material, effects of machining parameters on AOC values have been investigated and the most effective

Fig. 5 Surface plot of AOC (μm) versus I (A), P (bar) and N (rpm)
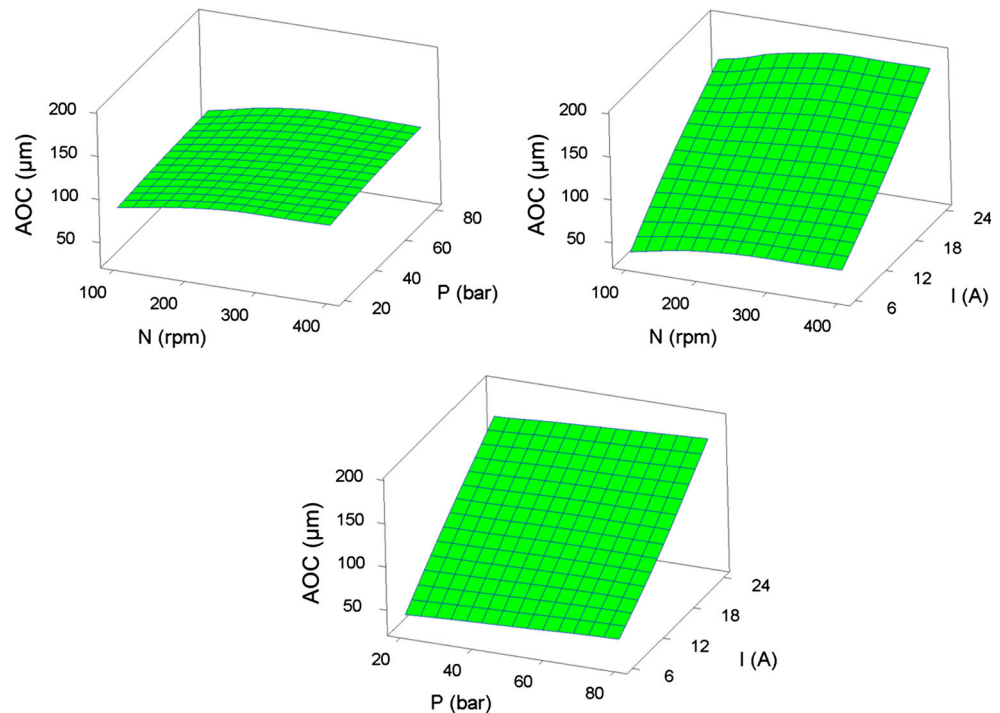
machining parameters for yielding low AOC values have been determined.

Figure 5 shows graphical depictions of the change in AOC values calculated using the measurements of the diameters of micro-holes drilled as part of the tests conducted, in response to the machining parameters used. Analysis of Fig. 5 shows that, without exception, AOC values increase rapidly as discharge current is increased, indicating hole diameters larger than electrode tool diameters. This is as expected per the fundamental principles of EDM, as increased discharge current leads to more powerful sparking between the electrode tool and the workpiece, which in turn enables a larger hole diameter [5]. It has been determined that to obtain micro-holes using EDM which conform to electrode tool diameters, discharge current values should be kept lower.

The effects on AOC, of the rpm values used for electrode rotation, as well as the dielectric fluid pressure values, were investigated, and the results, as can be observed in Fig. 5, indicate that increases in electrode tool rpm and dielectric fluid pressure cause an increase in AOC values. Increased electrode tool rotation rpm and dielectric fluid pressure have allowed an increased flow of clean dielectric fluid to the machining region and also enabled residual particles to be better flushed away, and consequently have resulted in more effective sparking. This has resulted in sustained sparking, leading to increased erosion and thereby, increased AOC values.

Taper angle (TA) is another indicator for evaluating hole profile accuracy in EDM micro-hole drilling. The TA value

is obtained by taking the difference of entrance and exit hole diameters and dividing by the length of the hole. Figure 6 shows graphical depictions of the change in TA values calculated using the measurements of the diameters of micro-holes drilled as part of the tests conducted, in response to the machining parameters used. Analysis of Fig. 6 shows that the TA value increases as discharge current, rpm and dielectric fluid pressure values increase. It is considered that the same factors acting to increase AOC values (described earlier) also lead to an increase in TA values.

A review of the results obtained for AOC and TA values indicates that increases in discharge current, dielectric fluid pressure and electrode tool rpm values cause a sustained increase in AOC and TA values. This is an undesirable outcome in EDM micro-hole drilling operations and is among the outstanding problems awaiting solution.

To provide a solution to the problem, certain studies have used electrodes with insulation [26]; however, due to high temperatures experienced during machining, chemical structure of the insulating material broke down, failing to prevent increases in AOC and TA values.

Accordingly, to obtain reasonable AOC and TA values in EDM micro-hole drilling operations, careful specification of machining parameters is required.

3.4 ANOVA

In order to obtain detailed information about the effect of input parameters including discharge current, dielectric

Fig. 6 Surface plot of TA (°) versus I (Å), P (bar) and N (rpm)
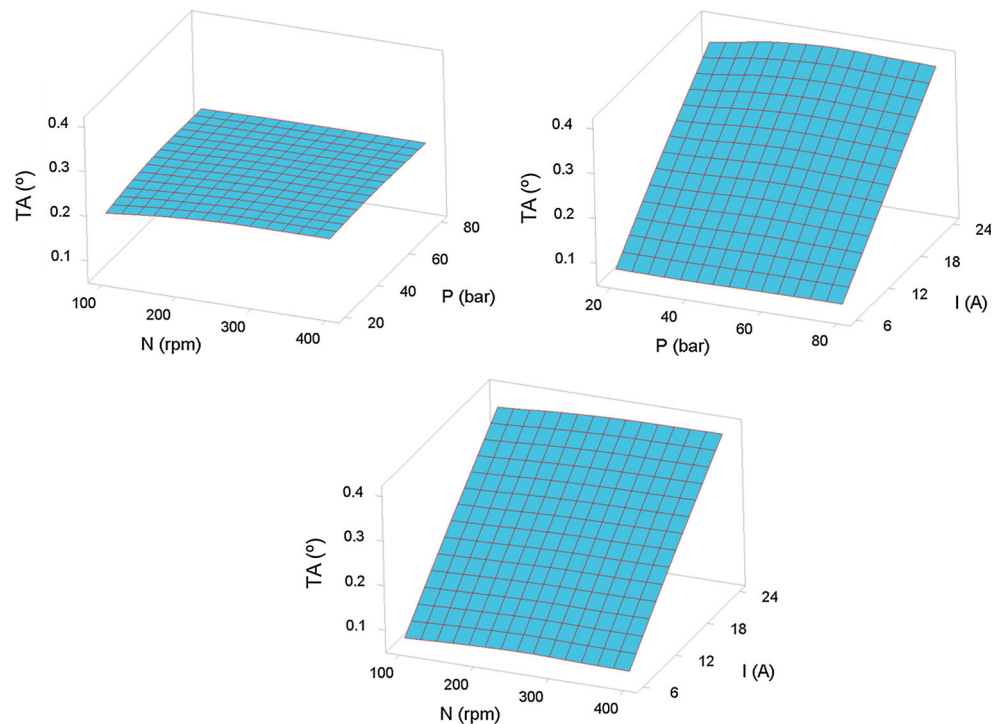
liquid pressure and electrode tool rotational speed on experimental results such as machining rate, electrode wear rate, average over-cut and taper angle, analysis of variance was carried out. It also determined significant parameters and insignificant parameters in responses by using F values of each independent parameter [27]. The influence of input parameters on output characteristics is seen in the last column of the ANOVA table. In present study, ANOVA was carried out by 95% confidence level and 5% significance level and it was tabulated as seen in Table 3. According to Table 3, discharge current, dielectric liquid pressure and electrode tool rotational speed influenced machining rate by 94 3.8 and 0.6%, respectively, and error can be given as 1.7%. From Table 3, discharge current, dielectric liquid pressure and electrode tool rotational speed influenced electrode wear rate by 98.4, 0.3 and 0.5%. Further, these process parameters affected the average over-cut by 96.6, 0.5, and 2.3% and they affected taper angle by 99.3, 0.1 and 0.1%. Therefore, discharge current was the most important parameter affecting the machining rate, electrode wear rate, average over-cut and taper angle. According to Table 3, it was demonstrated that discharge current and tool rotational speed had statistical and physical significance on electrode wear rate and taper angle at the reliability level by 95% as their P value results are lower than 0.05. Further, while all process parameters had statistical and physical significance on average over-cut, discharge current and dielectric liquid pressure had statistical and physical significance on machining rate.

3.5 Predictive modeling with RA and ANNs

After experimental analysis in order to write predictive models, test results in micro-deep EDM drilling of AISI 304 stainless steel were utilized using regression analysis via Minitab 17.0 software. Nowadays, regression analysis is commonly used by researchers to determine the relationship between the process parameters and output(s) [28]. In the current study, regression analysis based on linear model (first order model) was used for predictive models. Control factors or independent parameters used in this study were discharge current (I), dielectric liquid pressure (P) and electrode tool rotational speed (N) and responses or dependent parameters were machining rate (MR), electrode wear rate (EWR), average over-cut (AOC) and taper angle (TA). According to linear regression analysis, estimated model for machining rate, electrode wear rate, average over-cut and taper angle can be expressed by the following Eqs. (3–6):

$$\text{MR (mg/min)} = -21.4431 + 2.91077 \times \text{I (Å)} + 0.154177 \times \text{P (bar)} + 0.0128313 \times \text{N (rpm)} \tag{3}$$

$$\text{EWR (mg/min)} = -8.11454 + 1.20087 \times \text{I (Å)} - 0.0175472 \times \text{P (bar)} + 0.00530341 \times \text{N (rpm)} \tag{4}$$

$$\text{AOC (μm)} = -17.1481 + 6.96561 \times \text{I (Å)} + 0.148016 \times \text{P (bar)} + 0.0600794 \times \text{N (rpm)} \tag{5}$$

Table 3 Results of ANOVA analysis

Variation of source	Degree of freedom (DF)	Sum of squares (SS)	Mean of squares (MS)	F ratio	P value	Contribution (%)
MR						
Discharge current	2	12,811.0	6405.5	566.96	0.000	94
Dielectric liquid pressure	2	511.8	255.9	22.65	0.000	3.8
Rotational speed	2	75.1	37.6	3.33	0.057	0.6
Error	20	226.0	11.3			1.7
Total	26	13,623.9				100
EWR						
Discharge current	2	2204.97	1102.48	1144.66	0.000	98.4
Dielectric liquid pressure	2	5.62	2.81	2.92	0.077	0.3
Rotational speed	2	12.06	6.03	6.26	0.008	0.5
Error	20	19.26	0.96			0.9
Total	26	2241.90				100
AOC						
Discharge current	2	73,365	36,682	1665.42	0.000	96.6
Dielectric liquid pressure	2	370	185	8.40	0.002	0.5
Rotational speed	2	1770	885	40.19	0.000	2.3
Error	20	441	22			0.6
Total	26	75,946				100
TA						
Discharge current	2	0.445096	0.222548	2507.20	0.000	99.3
Dielectric liquid pressure	2	0.000537	0.000268	3.02	0.071	0.1
Rotational speed	2	0.000688	0.000344	3.87	0.038	0.1
Error	20	0.001775	0.000089			0.4
Total	26	0.448095				100

$$\begin{aligned} \text{TA}\,(\theta) = &\tan^{-1}(-0.00065787 + 0.000299438 \times \text{I}\,(\text{Å}) \\ &+ 2.44802\text{e}-006 \times \text{P}\,(\text{bar}) \\ &+ 6.4246\text{e}-007 \times \text{N}\,(\text{rpm})) \end{aligned}$$
(6)

In addition, artificial neural network (ANN) method is also widely employed in the variety of fields [29–33]. There are some algorithms such as Levenberg–Marquardt (LM), Bayesian regularization (BR) and scaled conjugate gradient (SCG) algorithms for neural network training. These algorithms have different advantages according to each other [34]. Because LM algorithm operates quicker once it trains a medium-sized feed forward neural network [34], in this study fermi transfer function based on the back-propagation learning with LM in ANNs model was used in order to obtain predictive models. There were three input parameters that were discharge current (I), dielectric liquid pressure (P) and electrode tool rotational speed (N) for each output, and desired outputs were MR, EWR, AOC and TA. ANNs were established in two phases including "training phase" and "propagation phase". For training phase while I, P and N were considered as input variables for each output, MR, EWR, AOC and TA were considered as output parameters. For propagation phase, ANNs were created according to four layers 3-6-5-1, 3-5-6-1, 3-4-5-1 and 3-6-5-1 containing input layer, two hidden layers and output for MR, EWR, AOC and TA, respectively, as shown in Fig. 7. ANNs were trained through obtained 21 test outputs and then it was verified and tested through six test outputs. Since normalization is necessary so that selected inputs are at a comparable range, input and output values were normalized at range between 0 and 1 by following Eq. (7):

$$N_{\text{v}} = \left[\frac{N_i - N_{\text{min}}}{N_{\text{max}} - N_{\text{min}}} \right]$$
(7)

In Eq. (7), N_{v} is normalization value, N_i is input value, N_{min} is minimum value, and N_{max} is maximum value.

Predictive models obtained from the ANNs model so as to estimate the outputs including MR, EWR, AOC and TA can be expressed, respectively, as following Eqs. (8–11):

$$N_{\mathrm{MR}} = \left(1 + e^{-4(-1.550154 \times N_7 + 1.345999 \times N_8 - 1.428762 \times N_9 - 1.303692 \times N_{10} + 1.028064 \times N_{11} - 0.5)}\right)^{-1} \tag{8}$$

$$N_{\mathrm{EWR}} = \left(1 + e^{-4(-0.702248 \times N_6 - 0.463843 \times N_7 - 1.886919 \times N_8 - 0.849448 \times N_9 + 0.399743 \times N_{10} + 1.905267 \times N_{11} - 0.5)}\right)^{-1} \tag{9}$$

$$N_{\mathrm{TOC}} = \left(1 + e^{-4(-0.781303 \times N_5 + 1.972745 \times N_6 - 1.158786 \times N_7 + 1.607220 \times N_8 - 1.338764 \times N_9 - 0.5)}\right)^{-1} \tag{10}$$

$$N_{\mathrm{TA}} = \tan^{-1}\left(\left(1 + e^{-4(1.769993 \times N_7 - 1.644160 \times N_8 - 0.886305 \times N_9 - 1.461106 \times N_{10} + 0.248677 \times N_{11} - 0.5)}\right)^{-1}\right) \tag{11}$$

Fermi transfer function used in predictive equations was written by following Eq. (12):

$$N_{(i)} = \frac{1}{1 + e^{-4x(E_i - 0.5)}}. \tag{12}$$

In Eq. (12) in order to calculate E_i values for level 1 neurons, Eq. (13) can be written as following:

$$E_i = w_{1i}xI + w_{2i}xP + w_{3i}xN. \tag{13}$$

E_i values for level 2 neurons were calculated by Eq. (14). In these equations mentioned above, i indicates neuron number.

$$E_i = w_{1i}xN_1 + w_{2i}xN_2 + w_{3i}xN_3 + \cdots\cdots + w_{ii}xN_i. \tag{14}$$

In order to calculate the reliability of written models, the determination coefficient expressed as R^2 was used for theoretical analysis of models. It is recommended that R^2 should be between 0.8 and 1 [35]. In present work, the value of the determination coefficient obtained from regression equations for MR, EWR, AOC and TA was $R^2 = 99.77, 98.14, 98.72$ and 95.79%. R^2 value obtained from ANNs equations for MR, EWR, AOC and TA was calculated as 99.88, 99.66, 99.43 and 99.41%, respectively. A comparison between measured experiments values and predicted values with help of ANNs and RA was graphically conducted as shown in Fig. 8. According to confirmation test result, it can be said that results obtained from equations were normally distributed. Due to high R^2 value of model and confirmation test results, written mathematical models through both ANNs and RA can be used for prediction of the results in micro-drilling with EDM of AISI 304 stainless steel. When an evaluation was conducted for linear regression analysis and artificial neural networks, it could be said that all ANN models were suitable so as to obtain the estimated results in terms of both theoretical analysis and graphical analysis.

3.6 Mono-and multiple response optimization

#### 3.6.1 Mono-optimization with S/N analysis

In order to find the optimum levels of EDM input parameters, signal-to-noise (S/N) analysis was performed using Minitab software. The data "signal" exhibits the desired influence, and data "noise" exhibits the undesired effect on outputs. Hence, maximum S/N ratio is calculated in order to obtain optimum points. S/N ratios can be calculated with three different methods such as nominal-the-best, smaller-the-better and larger-the-better. In current study, while S/N ratios for MR were determined with larger-the-better calculation method and ratios for EWR, AOC and TA were calculated with smaller-the-better calculation method by following Eqs. (15) and (16) [27]:

$$\text{For EWR, AOC and TA, } \mathrm{S/N_{SB}} = -10\log\left(\frac{1}{n}\sum_{i=1}^{n} r_i^2\right). \tag{15}$$

$$\text{For MR, } \mathrm{S/N_{LB}} = -10\log\left(\frac{1}{n}\sum_{i=1}^{n} \frac{1}{r_i^2}\right). \tag{16}$$

In Eqs. (15) and (16), r_i is the measured value of output for ith experiment and n is the test number made in this study.

Figure 9 shows the graphic of mean of S/N ratios for outputs. According to S/N graphic, it is understood that the highest S/N ratio provides the optimum levels. As seen in Fig. 9a, the optimum EDM drilling parameters, which were the discharge current of 24 Å, the dielectric liquid pressure of 80 bar and rotational tool speed of 400 rpm, were obtained for maximum MR value. As seen in Fig. 9b, the optimal parametric combination for EWR was determined to be I_1–P_3–N_1 which was as follows: discharge current of 6 Å, the dielectric liquid pressure of 80 bar and rotational tool speed of 100 rpm. In order to obtain minimum AOC and TA values, drilling parameter combination was I_1–P_1–
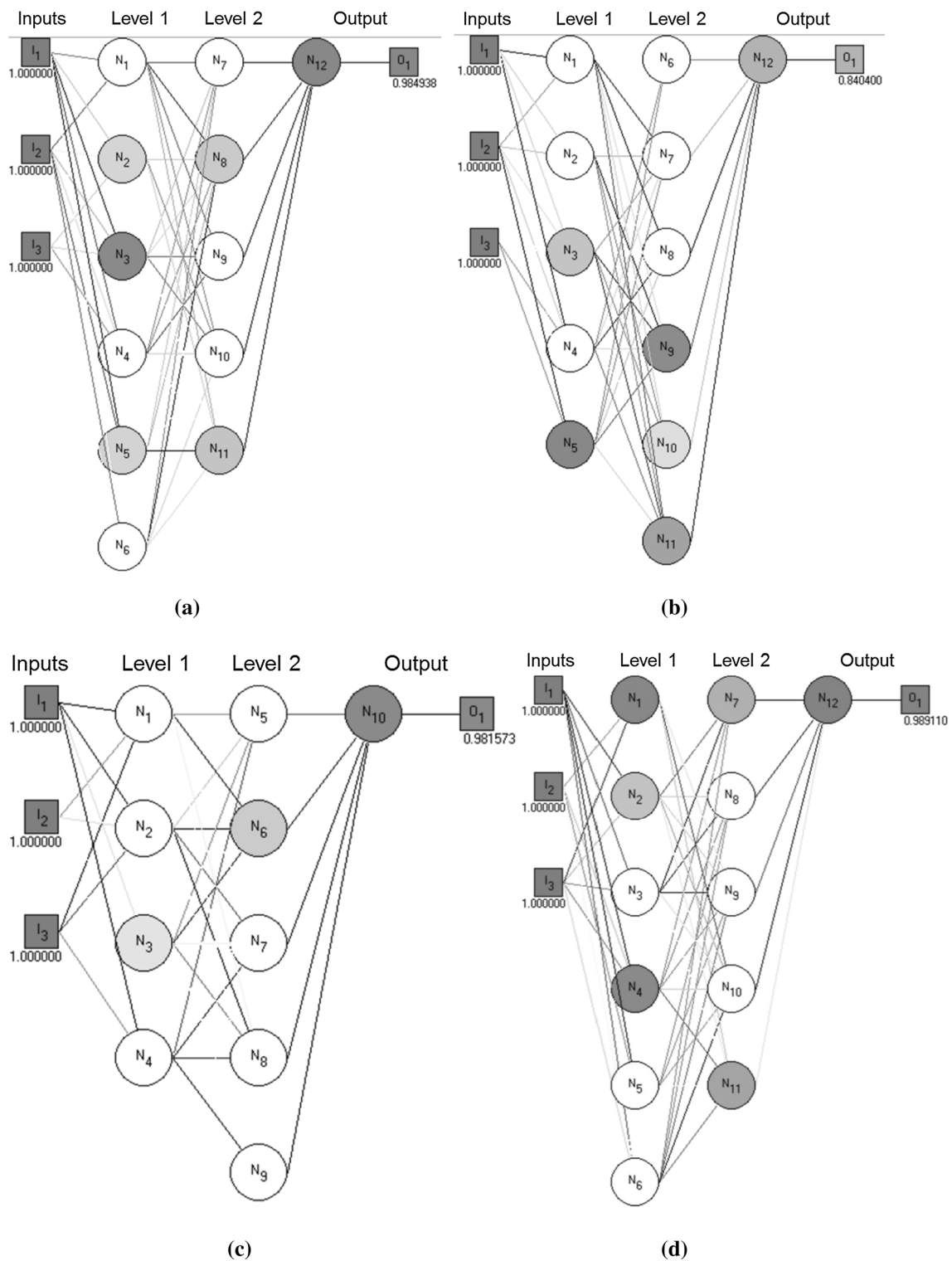
Fig. 7 ANN designs in LM algorithm for **a** MR, **b** EWR, **c** AOC and **d** TA

N_1 as seen in Fig. 9c, d. In addition, these graphics also demonstrated that discharge current was the most influential EDM drilling parameter for MR, EWR, AOC and TA

since the biggest difference between S/N ratios observed in discharge current. As mentioned above, this result was similar with ANOVA result.
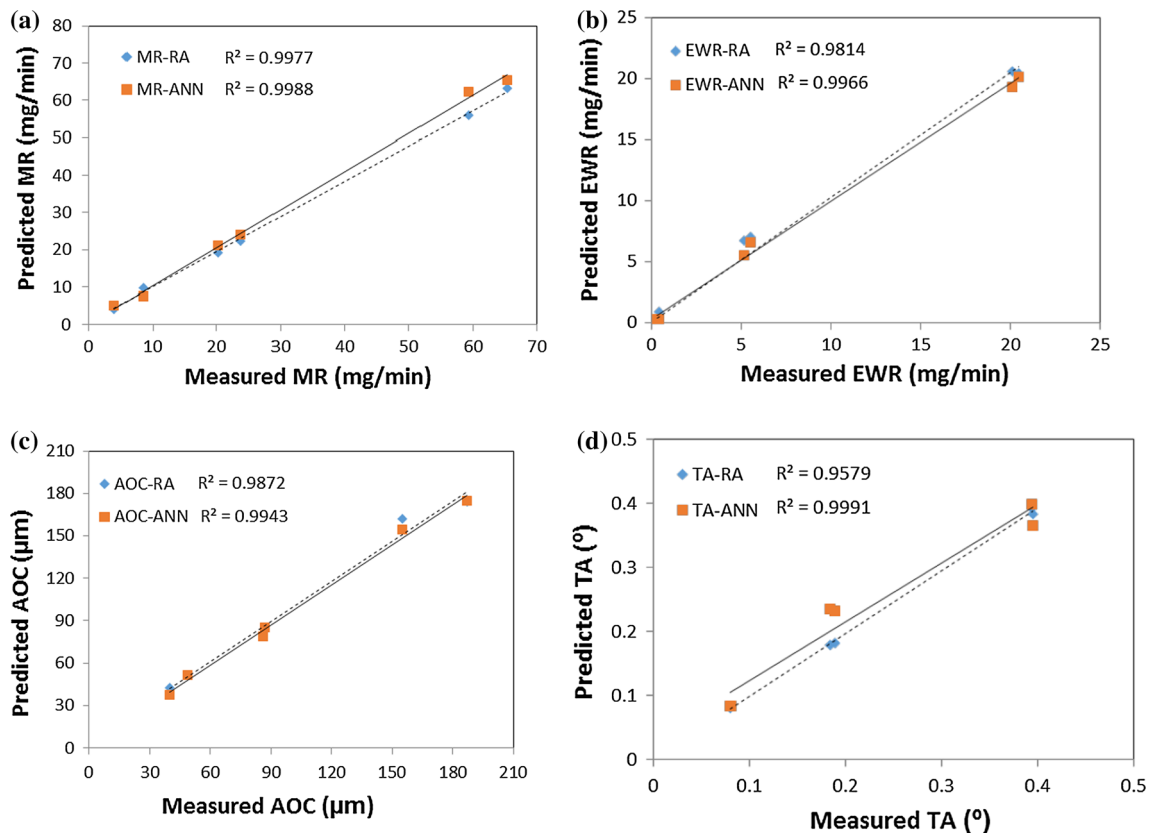
Fig. 8 Comparison between ANN and RA models. **a** MR, **b** EWR, **c** AOC and **d** TA

3.6.2 Multiple response optimization with RSM

In spite of high estimation accuracy by mono-optimization with S/N analysis, the optimum parameter combination for more than one output can be different [36]. Therefore, multi-response optimization is required for more suitable combination of control parameter. In order to determine simultaneously optimal outputs, response surface methodology (RSM) with desirability function analysis can be useful method in engineering applications [37]. In the desirability function analysis, the results are transformed into a dimensionless desirability value which is written as d [37]. This value is between $d = 0$ and $d = 1$. If $d = 0$ or close to 0, then the output is highly undesirable. If $d = 1$ or close to 1, then the response is wonderfully desirable. In this approach, there are three types of desirability analysis for different goals. These are: minimize the response, hit a target value and maximize the response [37]. In present study, the desirability function analysis for MR was performed with maximize the response method so as to achieve maximum MR value. Further, the desirability function analysis for EWR, AOC and TA was made according to minimize the response method since minimum EWR, AOC and TA were desired in micro-drilling with EDM of AISI 304 stainless steel. Optimization of

process parameters for multiple responses was simultaneously achieved using the desirability-based approach. Figure 10 shows the graph of desirability analysis so as to establish simultaneously maximum MR and minimum EWR, AOC and TA values. According to Fig. 10, the best results for MR, EWR, AOC and TA were found to be 20.98 mg/min (desirability value, $d = 0.2759$), 2.923 mg/min ($d = 0.8978$), 66.6164 μm ($d = 0.77115$) and 0.15147° ($d = 0.74361$) in levels of control factors that are current discharge of 10.1818 Å, dielectric liquid pressure of 58.7879 bar and electrode tool rotational speed of 100 rpm in EDM micro-deep drilling of AISI 304 stainless steel.

3.6.3 Confirmation experiments

In the last phase of the optimization made by S/N, confirmation tests have to be performed to check the reliability of the optimization [38]. The confirmation tests were made at the optimum points of the control factors assigned for MR, EWR, AOC and TA which are I_3–P_3–N_3, I_1–P_3–N_1, I_1–P_1–N_1 and I_1–P_1–N_1, respectively. In order to verify the confirmation, test results were analyzed by taking into account the confidence interval (CI) calculated using following Eqs. (17) and (18).
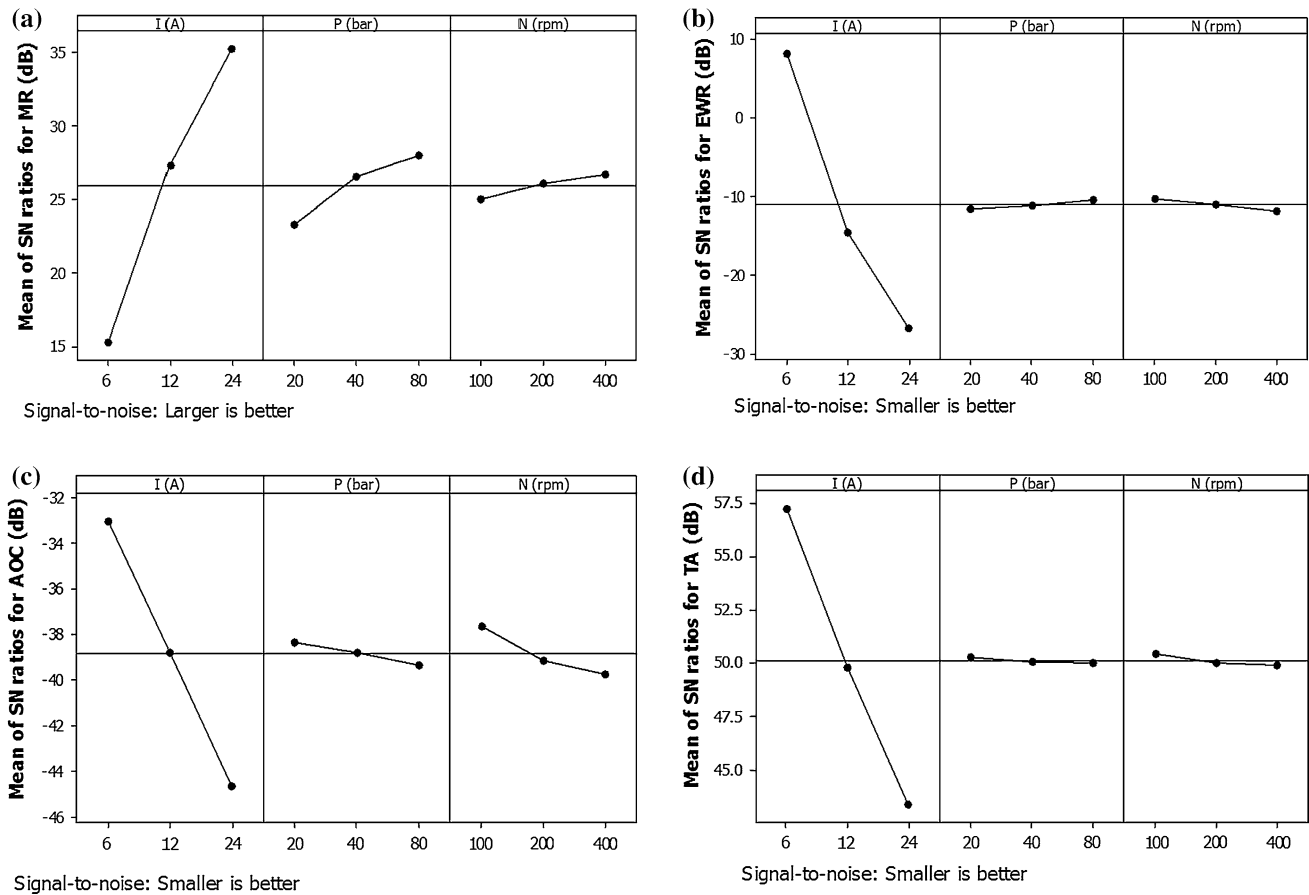
Fig. 9 Mean of S/N ratios for **a** MR, **b** EWR, **c** AOC and **d** TA

$$CI = \sqrt{F_{\alpha;1;Ve} \times V_{ep} \times \left(\frac{1}{n_{eff}} + \frac{1}{R} \right)} \qquad (17)$$

$$n_{eff} = \frac{N}{1 + T_{dof}} \qquad (18)$$

In Eq. (17), $F_{\alpha,1,Ve}$ is the F ratio at 95% confidence level, α is the significance level, V_e is the degrees of freedom of error, V_{ep} is error variance, n_{eff} is the effective number of replications, R is the number of replications for verification test. In Eq. (18), N is the total number of tests, and T_{dof} is the total main factor degrees of freedom.

According to F test table, $F_{\alpha,1,20}$ is 4.35. Further, R is 3, N is 27, T_{dof} is 6, and V_{ep} is 11.30, 0.96, 22 and 0.000089 for MR, EWR, AOC and TA. Based on these values, n_{eff} and CI were calculated for each output using Eqs. (17) and (18). As seen in Table 4 it can be said clearly that the difference between calculated values and experimental values is less than the confidence interval of each output parameter. Therefore, optimization was finalized successfully at a significance level of 0.05 in micro-electrical discharge drilling of AISI 304 stainless steel.
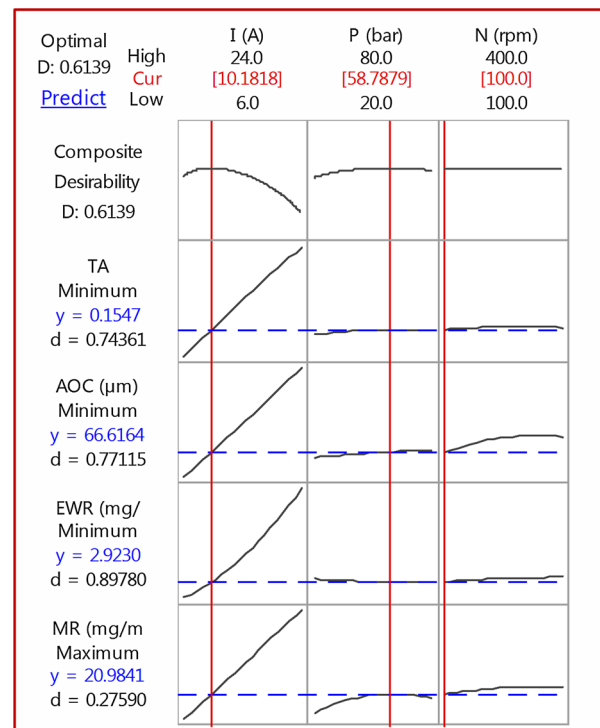

Fig. 10 Plot of multiple response optimization

Table 4 Confirmation test results

Output	Confirmation test result	Calculated value	Difference	Confidence interval	Optimization
MR	69.231	64.78	4.45	5.40	Successful
EWR	0.262	0.183	0.079	1.57	Successful
AOC	30	30.8519	0.8519	7.53	Successful
TA	0.0750	0.0658	0.0092	0.0151	Successful

4 Conclusion

The results for current work can be listed as below:

- An important increase in MR values was observed in response to increase in discharge current. With increased discharge energy, more material was melted and vaporized in unit time from the surface of the workpiece material.
- An increase in both electrode rotation rpm and dielectric spray pressure was found to increase MR values when machining AISI-304 type stainless steel material. The resulting increase has been significant in terms of machining performance and savings, allowing the drilling of micro-holes to be completed in shorter durations.
- While EWR values were increased as discharge current and tool rotational speed were increased, decreased EWR values were observed in relation to increases in dielectric spray pressure. This decrease in EWR values observed in relation to increased dielectric spray pressure is interpreted to be due to the more effective means of washing and cooling that were enabled.
- AOC and TA values increase rapidly as discharge current is increased, indicating hole diameters larger than electrode tool diameters. This is as expected per the fundamental principles of EDM. Increases in electrode tool rpm and dielectric fluid pressure cause an increase in AOC values.
- According to ANOVA result, discharge current was the most important factor affecting the machining rate, electrode wear rate, average over-cut and taper angle. Discharge current and tool rotational speed had statistical significance on electrode wear rate and taper angle. Further, while all process parameters had statistical significance on average over-cut, discharge current and dielectric liquid pressure had statistical significance on machining rate.
- Mathematical models obtained through both ANNs and RA can be used for prediction of the results in micro-drilling with EDM of AISI 304 stainless steel. When an evaluation was conducted for linear regression analysis and artificial neural networks, it could be said that all ANN models were suitable so as to obtain the estimated results in micro-deep hole EDM-drilling of AISI 304 stainless steel.
- Optimum process parameters for mono-output, the discharge current of 24 Å, the dielectric liquid pressure of 80 bar and rotational tool speed of 400 rpm, were obtained for maximum MR value. Optimal parametric combination for EWR was found to be I_1–P_3–N_1 which was as follows: discharge current of 6 Å, the dielectric liquid pressure of 80 bar and rotational tool speed of 100 rpm. In order to obtain minimum AOC and TA values, drilling parameter combination was I_1–P_1–N_1. Further, confirmation tests showed that optimization is successful.
- Optimum process parameters, which were discharge of 10.1818 Å, dielectric liquid pressure of 58.7879 bar and electrode tool rotational speed of 100 rpm, for multiple responses were determined through RSM with desirability function in EDM micro-deep drilling of AISI 304 stainless steel.

References

1. Meral G, Sarıkaya M, Dilipak H, Şeker U (2015) Multi-response optimization of cutting parameters for hole quality in drilling of AISI 1050 steel. Arab J Sci Eng 40(12):3709–3722
2. Chow HM, Lee SM, Yang LD (2008) Machining characteristic study of friction drilling on AISI 304 stainless steel. J Mater Process Technol 207(1):180–186
3. Kuram E, Ozcelik B (2013) Multi-objective optimization using Taguchi based grey relational analysis for micro-milling of Al 7075 material with ball nose end mill. Measurement 46(6):1849–1864
4. Yılmaz V, Sarıkaya M, Dilipak H (2015) Deep micro-hole drilling for Hadfield steel by electro-discharge machining (EDM). Mater Technol 49(3):377–386
5. Kuppan P, Rajadurai A, Narayanan S (2008) Influence of EDM process parameters in deep hole drilling of Inconel 718. Int J Adv Manuf Technol 38(1–2):74–84
6. Ay M, Çaydaş U, Hasçalık A (2013) Optimization of micro-EDM drilling of Inconel 718 superalloy. Int J Adv Manuf Technol 66(5–8):1015–1023
7. Asokan T, Reddy SS, Costa PDE (2000) Electrical discharge drilling of titanium alloys for aerospace applications. In:

Proceedings of 19th AIMTDR conference. IIT Madras, Chennai, pp 161–165

8. Mohan B, Rajadurai A, Satyanarayana KG (2002) Effect of SiC and rotation of electrode on electric discharge machining of Al–SiC composite. J Mater Process Technol 124:297–304

9. Mohan B, Rajadurai A, Satyanarayana KG (2004) Electric discharge machining of Al–SiC metal matrix composites using rotary tube electrode. J Mater Process Technol 153–154:978–985

10. Puertas I, Luis CJ, Alvarez L (2004) Analysis of the influence of EDM parameters on surface quality, MRR and EW of WC–Co. J Mater Process Technol 153:1026–1032

11. Lee CS, Heo EY, Kim JM, Choi IH, Kim DW (2015) Electrode wear estimation model for EDM drilling. Robot Comput-Integr Manuf 36:70–75

12. Plaza S, Sanchez JA, Perez E, Gil R, Izquierdo B, Ortega N, Pombo I (2014) Experimental study on micro EDM-drilling of Ti–6Al–4V using helical electrode. Precis Eng 38(4):821–827

13. Jahan MP, San Wong Y, Rahman M (2010) A comparative experimental investigation of deep-hole micro-EDM drilling capability for cemented carbide (WC–Co) against austenitic stainless steel (SUS 304). Int J Adv Manuf Technol 46(9–12):1145–1160

14. Pradhan BB, Masanta M, Sarkar BR, Bhattacharyya B (2009) Investigation of electro-discharge micro-machining of titanium super alloy. Int J Adv Manuf Technol 41(11–12):1094–1106

15. Wang D, Zhao WS, Gu L, Kang XM (2011) A study on micro-hole machining of polycrystalline diamond by micro-electrical discharge machining. J Mater Process Technol 211(1):3–11

16. Sarıkaya M, Yılmaz V, Dilipak H (2016) Modeling and multi-response optimization of milling characteristics based on Taguchi and gray relational analysis. Proc Inst Mech Eng Part B J Eng Manuf 230(6):1049–1065

17. Sarıkaya M, Güllü A (2014) Taguchi design and response surface methodology based analysis of machining parameters in CNC turning under MQL. J Clean Prod 65:604–616

18. Davoodi B, Eskandari B (2015) Tool wear mechanisms and multi-response optimization of tool life and volume of material removed in turning of N-155 iron–nickel-base superalloy using RSM. Measurement 68:286–294

19. Joardar H, Das NS, Sutradhar G, Singh S (2014) Application of response surface methodology for determining cutting force model in turning of LM6/SiC P metal matrix composite. Measurement 47:452–464

20. Moghaddam TB, Soltani M, Karim MR, Baaj H (2015) Optimization of asphalt and modifier contents for polyethylene terephthalate modified asphalt mixtures using response surface methodology. Measurement 74:159–169

21. Mukherjee I, Ray PK (2006) A review of optimization techniques in metal cutting processes. Comput Ind Eng 50(1):15–34

22. Pham DT, Dimov SS, Bigot S, Ivanov A, Popov K (2004) Micro-EDM-recent developments and research issues. J Mater Process Technol 149(1):50–57

23. Yan BH, Wang CC (1999) The machining characteristics of Al₂O₃/6061Al composite using rotary electro-discharge machining with a tube electrode. J Mater Process Technol 95:107–111

24. Chen SL, Yan BH, Huang FY (1999) Influence of kerosene and distilled water as dielectrics on the electric discharge machining characteristics of Ti–6Al–4V. J Mater Process Technol 87:107–111

25. Ho KH, Newman ST (2003) State of the art electrical discharge machining (EDM). Int J Mach Tools Manuf 43:1287–1300

26. Ferraris E, Castiglioni V, Ceyssens F, Annoni M, Lauwers B, Reynaerts D (2013) EDM drilling of ultra-high aspect ratio micro holes with insulated tools. CIRP Ann Manuf Technol 62(1):191–194

27. Kıvak T, Samtaş G, Çiçek A (2012) Taguchi method based optimisation of drilling parameters in drilling of AISI 316 steel with PVD monolayer and multilayer coated HSS drills. Measurement 45(6):1547–1557

28. Sarıkaya M, Güllü A (2015) Multi-response optimization of MQL parameters using Taguchi based GRA in turning of difficult-to-cut alloy Haynes 25. J Clean Prod 91:347–357

29. Korkut I, Acır A, Boy M (2011) Application of regression and artificial neural network analysis in modelling of tool–chip interface temperature in machining. Expert Syst Appl 38(9):11651–11656

30. Karabulut Ş (2015) Optimization of surface roughness and cutting force during AA7039/Al₂O₃ metal matrix composites milling using neural networks and Taguchi method. Measurement 66:139–149

31. Karabulut Ş, Karakoç H (2015) Investigation of surface roughness in the milling of Al7075 and open-cell SiC foam composite and optimization of machining parameters. Neural Comput Appl. doi:10.1007/s00521-015-2058-x

32. Mia M, Dhar NR (2016) Response surface and neural network based predictive models of cutting temperature in hard turning. J Adv Res 7(6):1035–1044

33. Mia M, Khan MA, Dhar NR (2016) Performance prediction of high-pressure coolant assisted turning of Ti–6Al–4V. Int J Adv Manuf Technol. doi:10.1007/s00170-016-9468-5

34. Mia M, Dhar NR (2016) Prediction of surface roughness in hard turning under high pressure coolant using artificial neural network. Measurement 92:464–474

35. Cetin MH, Ozcelik B, Kuram E, Demirbas E (2011) Evaluation of vegetable based cutting fluids with extreme pressure and cutting parameters in turning of AISI 304L by Taguchi method. J Clean Prod 19:2049–2056

36. Mia M, Khan MA, Rahman SS, Dhar NR (2016) Mono-objective and multi-objective optimization of performance parameters in high pressure coolant assisted turning of Ti–6Al–4V. Int J Adv Manuf Technol. doi:10.1007/s00170-016-9372-z

37. Ezilarasan C, Kumar VSS, Velayudham A (2013) An experimental analysis and measurement of process performances in machining of Nimonic C-263 super alloy. Measurement 46(1):185–199

38. Sarikaya M (2015) Optimization of the surface roughness by applying the Taguchi technique for the turning of stainless steel under cooling conditions. Mater Tehnol 49(6):941–948